Supporting Information

Molatore et al. 10.1073/pnas.1003956107

SI Materials and Methods

Rat Tissue Samples. Rat tissues were snap-frozen in liquid nitrogen and stored at −80 °C until use. Histological examination by an experienced pathologist (A.P.) confirmed the diagnosis of hyperplasia or pheochromocytoma based on established criteria for rat adrenal medullary lesions (1): diffuse hyperplastic lesions showed a clear demarcation of cortex and medulla and the preservation of the reticulin meshwork. In pheochromocytoma the organization of the adrenal gland observed in wild-type animals was replaced by the appearance of tumor nodules that displaced the cortex (2). Large tumors showed blood pools, and reticulin stains revealed no reticulin within the tumors. Cryosections of adrenal tissues were macrodissected under a stereomicroscope M5-52765 (Wild) to remove the cortex. This approach gave us samples largely devoid of cortical cells, as previously demonstrated (2).

RNA Isolation and Microarray Preparation. Frozen 20-μm sections of normal adrenal gland (control), and glands with hyperplasia and tumors were obtained in a cryostat at −20 °C. Then, frozen tissue sections were applied on microscope slide SuperFrost (Roth) and adrenal medullary tissue was collected by macrodissection to eliminate the cortex. Normal adrenal RNA consisted of two pooled macrodissected adrenal medulla (one for each sex) from young wild-type rats (3 mo of age) or from adult rats (7 mo of age). Each pool contained RNA from three independent animals. Macrodissected samples were collected in test tubes and processed according to the protocol reported in Chomczynski and Sacchi (3). Total RNA used for microarrays was further purified by using the RNeasy Mini Kit (Qiagen). The quality of the RNA was assessed by RNA 6000 Pico Chip Kit (Agilent) and only high-quality RNA (RIN ≥7) was used for microarray analysis. For hyperplastic samples from 3-mo-old mutant rats, total RNA (2 μg) was amplified using the One-Cycle Target Labeling kit (Affymetrix); the larger samples from older animals with tumors (8–11 mo) were amplified with the MessageAmp II-Biotin Enhanced single round aRNA Amplification Kit (Ambion) with 120 ng total RNA as input. Ten micrograms of amplified aRNA were hybridized on Affymetrix Rat Genome 230 2.0 arrays containing about 31,000 probe sets. Labeling and scanning was done according to the Affymetrix expression protocol. In total, 16 samples were analyzed (3 mo of age: eight mutant/two wild-type pooled samples; 8–11 mo: four mutant/two wild-type pooled samples). Microarray data have been deposited in the Gene Expression Omnibus (GEO) database, www.ncbi.nlm.nih.gov/geo (accession no. GSE21006).

Microarray Analysis. Gene expression levels were estimated from probe intensities using the robust multiarray analysis method after quantile normalization and background correction (4). To eliminate any technical variation a batch effect removal procedure, based on analysis of variance, was performed using the Partek Genomic Suite (Partek, Inc.) software. To identify genes differentially expressed between hyperplasia and controls, or between tumors and controls, we performed gene filtering using SAM (Significance Analysis of Microarrays) (5). By applying 200 permutations, with a threshold of $\delta = 0.776$ and 1.272, respectively, SAM provided a filtered list of 363 genes that show at least over twofold change up-regulation ($n = 198$) or down-regulation ($n = 165$) in hyperplasia and a set of 489 genes up-regulated ($n = 183$) or down-regulated ($n = 306$) in pheochromocytoma, with a false-discovery rate of 1.18 and 1.19%. Heatmaps and dendrograms were prepared in CARMAweb (6).

Pathway Analysis. To gather insights into the most overrepresented dysregulated biological processes in our datasets, we used the Database for Annotation, Visualization and Integrated Discovery (DAVID) (http://david.abcc.ncifcrf.gov/summary.jsp). DAVID uses a unique agglomeration algorithm to condense a list of genes or associated biological terms into organized classes of related genes or biology, called biological modules. The Gene Functional Classification tool in DAVID builds clusters of genes with significantly similar ontologies as tested against the list of probe set identifications in the Affymetrix GeneChip Rat Genome 320 2.0 Array. For this analysis, the top 200 overexpressed probe set identifications in the lesions (at least twofold change compared with normal tissue) were used.

Key regulatory processes in tumor development were also identified using the Gene Ontology (GO) Tree Machine http://bioinfo.vanderbilt.edu/gotm/.

Real-Time qRT-PCR and RT-PCR in Rat Samples. We synthesized the first-strand cDNA from total mRNA using random hexamers and SuperScript II (Invitrogen). Quantitative RT-PCR for rat mRNA was done with TaqMan Inventoried primers and probes for rat *Cdkn2a*, *Cdkn2c*, *Sctr*, *Neurod1*, *Gal*, *Pqbp1*, *Cxcr4*, *Bmp7*, *Phox2a*, *L1cam*, and *Tcte1* genes, and for β2-microglobulin as internal control (Applied Biosystems). The assay for *Dgkh* was custom made. The assays were run as previously reported (7).

For RT-PCR of the *Tcte1* transcript, cDNA synthesis was performed as above. Then, we used the following primers for amplification: Fw: TTCACCTACCGAGACTGCC; Rev: TTGTGGGATAAGTCCAGCTC. These primers amplify a 164-bp fragment spanning the region between exon 2 and exon 3, the same region detected by the RealTime qRT-PCR assay Rn01757081_m1 used in Fig. 2.

Patients. The study was approved by the Ethics Committee of the Universities of Munich, Bern, Gliwice, and Florence and informed written consent was obtained from all patients. All patients had histologically confirmed adrenal or extra-adrenal pheochromocytomas (Table S2). Samples of tumor tissue were obtained from the core of the tumor (>80% tumor cells), were snap-frozen in dry-ice and then stored at –80 °C until processed. Phaeochromocytoma/paraganglioma patients studied included eight with MEN 2A, one with von Hippel-Lindau (VHL) syndrome, one with paraganglioma syndrome 1 (PGL1), one with PGL4, and a further 33 without evidence of an underlying hereditary condition for pheochromocytoma/paraganglioma (i.e., presumed sporadic). The diagnosis of VHL, MEN 2A, PGL1, or PGL4 was based on clinical and family history of multiple tumors characteristic of the particular disorder and confirmed by identification of underlying germ-line mutations of the the *RET* or the *SDHB* genes. Mutation in the *VHL* tumor suppressor gene was not identified in the patient with VHL phenotype. The PGL series of sporadic pheochromocytoma/paraganglioma was tested for germ-line *RET* mutations but none was found. Malignancy was defined based on the presence of distant metastases. Clinical data of the patients used for the qRT-PCR are shown in Table S2. Cases used for immunohistochemical staining are also indicated in Table S2 or were previously reported (8).

Human Tissues RNA Isolation and qRT-PCR. RNA from human snap-frozen pheochromocytoma tissue samples was extracted using the

TRIzol Protocol (Invitrogen). First-strand cDNA was synthesized from total mRNA as for the rat samples. Quantitative RT-PCR was done with TaqMan Inventoried primers and probes for human *GAL*, *DGKH*, *PHOX2A*, *L1CAM*, *BMP7*, *TCTE1 HASH1*/*ASCL1*, *SOX4*, and *EBF3* genes and for the *TBP* gene as internal control (Applied Biosystems). The assays were run as previously reported (7).

Western Blotting. For protein extraction from rat snap-frozen tissues, serial 50-μm tissue sections were resuspended in protein lysis buffer (10 mmol/L Tris-HCl pH 7.4, 5 mmol/L EDTA, 130 mmol/l NaCl, 1% Triton, and 1× Mini-Complete protease inhibitors mixture, Roche) and total proteins were extracted as reported (7). Equal protein amounts (50 μg) were resolved on 4 to 15% SDS/PAGE precast gels (Invitrogen) and blotted onto nitrocellulose membranes (Hybond-ECL; Amersham).

For protein extraction from frozen human tissues, normal adrenal medullary tissue cryosections (n = 3) were macrodissected to eliminate the cortex, pooled, and then resuspended in protein lysis buffer. Pheochromocytoma tissue fragments were cyrosectioned and resuspended in protein lysis buffer. Total protein extraction was performed as above.

Immunoblots were developed using West Pico chemoluminescent substrates (Pierce Chemical Company). Antibodies used were: anti-p27 monoclonal antibody (Transduction Laboratories), anti-L1CAM (Sigma Aldrich), and anti-Phox2A (SantaCruz Biotechnologies). To control for equal protein loading, α-tubulin immunostaining was performed (Sigma Aldrich).

Tissue Microarrays. Two tissue microarrays (TMA) were constructed from formalin-fixed paraffin-embedded tissues obtained from the archives of the Institute of Pathology, Technical University Munich, and of the Institute of Pathology, University of Bern. The first TMA was constructed by arraying 33 tissue cores, each of 1.5 mm diameter, and the second constructed by arraying 111 additional tissue cores of 0.6 mm diameter. Tissue cores were punched out of each donor block using a precision instrument (Beecher Instruments) and transferred to the recipient TMA blocks, as described elsewhere (9). The two TMAs contained a total of 144 neuroendocrine tumor (NET) tissue cores comprising: 130 gastro-entero-pancreatic NETs (62 ileum, 36 appendix, 9 duodenum, 8 pancreas, 5 colon, 5 liver, 3 stomach, 1 rectum, 1 gallbladder), 2 lung carcinoids, 2 bronchial carcinoids, 2 medullary thyroid cancers, 2 parathyroid adenomas, 4 paragangliomas (2 parasympathetic abdominal paragangliomas and 2 duodenal gangliocytic, nonchromaffin paragangliomas), and 2 pheochromocytomas.

Immunohistochemistry. Immunohistochemistry was performed on an automated immunostainer (Ventana Medical Systems) according to the manufacturer's protocols with minor modifications, as described elsewhere (9). Staining of 3-μm rat tissue sections was performed with antibodies against K_i-67 (BD Pharmingen; clone B56) and against phenylethanolamine N-methyltransferase (PNMT) (Enzo Life Science). Conventional 3-μm sections of human pheochromocytoma standard full section tissue blocks (n = 28) or of the two TMAs were used for immunohistochemistry. Staining was performed using a monoclonal antibody against L1CAM (1:200; Sigma). Images were recorded using a Hitachi camera HW/C20 installed in a Zeiss Axioplan microscope with Intellicam software (Zeiss MicroImaging). Scoring of the tissue immunoreactivity was performed by an experienced pathologist (A.P.) using the criteria commonly used in breast cancer patients to score for HER2/Neu immunoreactivity (DAKO Scoring) (10).

Statistical Analysis. Comparison between the top 200 nonredundant genes in Datasets S1 and S2 was performed using the program LOLA (List of Lists Annotated) (http://www.lola.gwu.edu/) (11). Reported in the text is the P value (= 3.73517E-128) we obtained. Comparison of the frequency of gene up-regulation by qRT-PCR between adrenal and extra-adrenal human pheochromocytoma was performed using both nonparametric Wilcoxon rank sum test and parametric t test (two-sided P value and one-sided P value was obtained for each test). Comparison between adrenergic and noradrenergic human tumors was performed using nonparametric Wilcoxon rank sum test and a t test after a log transformation.

1. Tischler AS, DeLellis RA (1988) The rat adrenal medulla. II. Proliferative lesions. *J Am Coll Toxicol* 7:23–44.
2. Shyla A, et al. (2010) Allelic loss of chromosomes 8 and 19 in MENX-associated rat pheochromocytoma. *Int J Cancer* 126:2362–2372.
3. Chomczynski P, Sacchi N (1987) Single-step method of RNA isolation by acid guanidinium thiocyanate-phenol-chloroform extraction. *Anal Biochem* 162:156–159.
4. Irizarry RA, et al. (2003) Summaries of Affymetrix GeneChip probe level data. *Nucleic Acids Res* 31:e15.
5. Tusher VG, Tibshirani R, Chu G (2001) Significance analysis of microarrays applied to the ionizing radiation response. *Proc Natl Acad Sci USA* 98:5116–5121.
6. Rainer J, Sanchez-Cabo F, Stocker G, Sturn A, Trajanoski Z (2006) CARMAweb: Comprehensive R- and bioconductor-based web service for microarray data analysis. *Nucleic Acids Res* 34(Web Server issue):W498–W503.
7. Pellegata NS, et al. (2006) Germ-line mutations in p27Kip1 cause a multiple endocrine neoplasia syndrome in rats and humans. *Proc Natl Acad Sci USA* 103:15558–15563.
8. Pellegata NS, et al. (2007) Human pheochromocytomas show reduced p27Kip1 expression that is not associated with somatic gene mutations and rarely with deletions. *Virchows Arch* 451:37–46.
9. Langer R, et al. (2006) Prognostic significance of expression patterns of c-erbB-2, p53, p16INK4A, p27KIP1, cyclin D1 and epidermal growth factor receptor in oesophageal adenocarcinoma: A tissue microarray study. *J Clin Pathol* 59:631–634.
10. Wolff AC, et al.; American Society of Clinical Oncology/College of American Pathologists (2007) American Society of Clinical Oncology/College of American Pathologists guideline recommendations for human epidermal growth factor receptor 2 testing in breast cancer. *Arch Pathol Lab Med* 131:18–43.
11. Cahan P, et al. (2005) List of lists-annotated (LOLA): A database for annotation and comparison of published microarray gene lists. *Gene* 360:78–82.

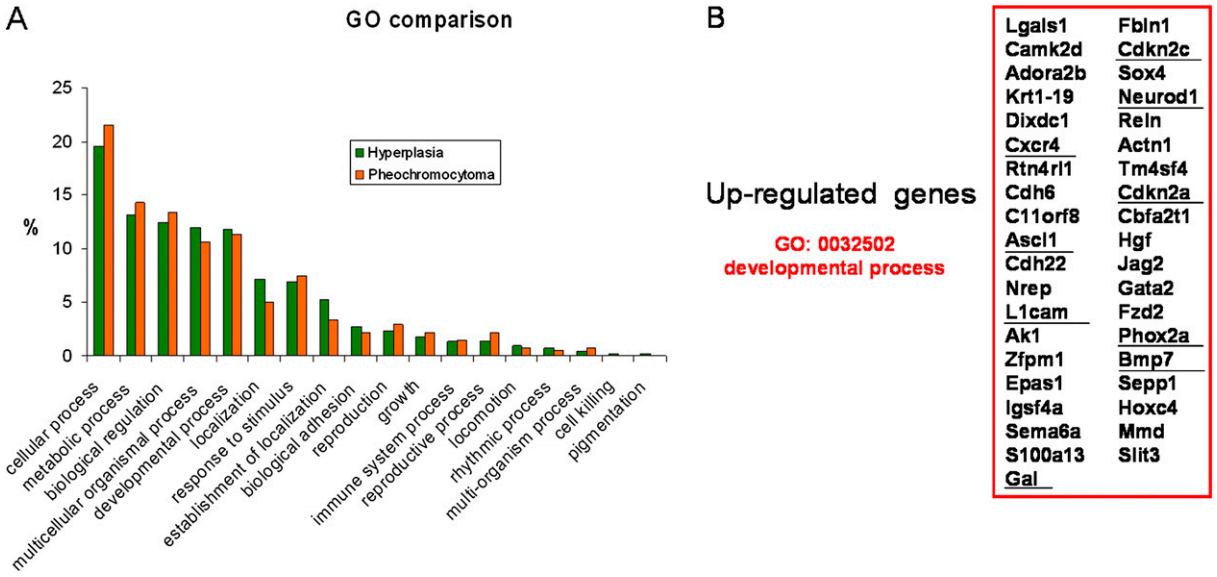

Fig. S1. Graphical representation of the distribution of the significantly dysregulated genes in rat lesions by functional category and list of genes belonging to the "Developmental Process" category. (*A*) The different functional categories are labeled along the *x* axis and the percentage of the recognized genes belonging to the various GO categories is indicated on the *y* axis. Functional categories were established based on the annotation provided by the GO database (http://www.geneontology.org) and are shown only for genes with known functions. The green bars represent values obtained for the adrenomedullary hyperplasia and the orange ones those for the pheochromocytoma. (*B*) List of genes belonging to the highly enriched GO category "Developmental Process" (GO: 0032502). Underlined are genes we validated by qRT-PCR in additional samples.

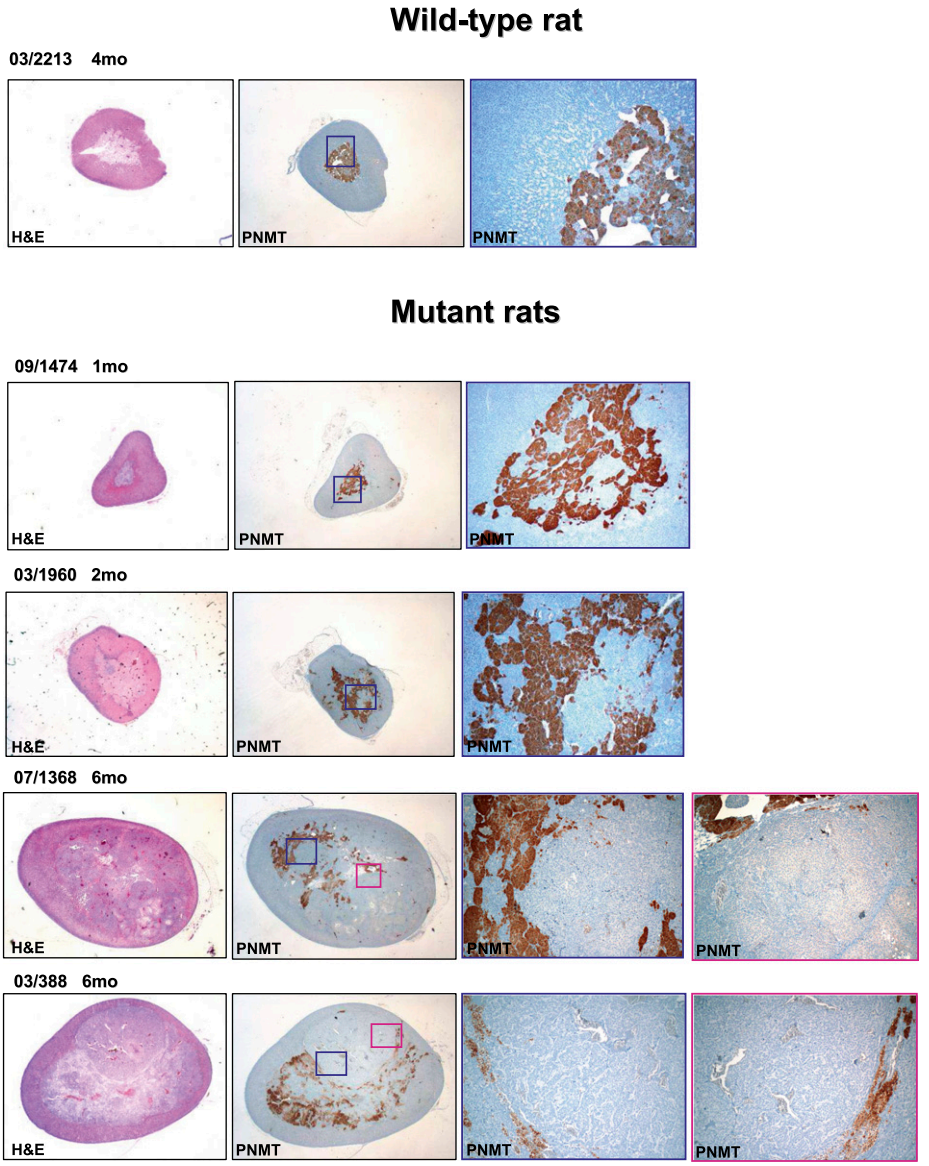

Fig. S2. Expression of PNMT in adrenal glands of unaffected and affected rats. Immunohistochemical staining of adrenal glands of a 4-mo-old wild-type mutant rat and of mutant rats at different ages (1, 2, 6, and 6 mo). Formalin-fixed, paraffin-embedded tissue sections of rat adrenal glands from the rats were stained with a specific anti-PNMT antibody. The tumor areas in older mutant rats (outlined) are composed of PNMT-negative cells. Original magnification: H&E 12.5×; (*Left*) PNMT: 12.5×; (*Right*) PNMT: 100×.

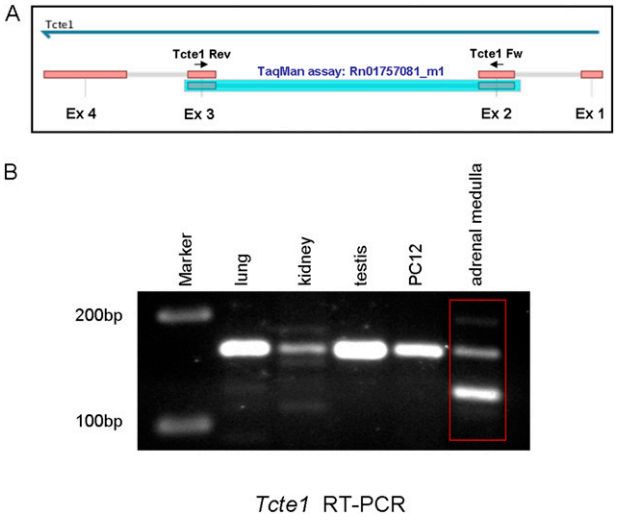

Fig. S3. RT-PCR for the *Tcte1* transcript in various rat tissues and in PC12 cells. (*A*) Schematic representation of the rat *Tcte1* gene with indicated the exons (Ex) and in blue the region targeted by the TaqMan qRT-PCR assay used in Fig. 3*A*. The primers we used for the RT-PCR (*B*) are indicated. (*B*) Total RNA was extracted from the indicated rat tissues or the PC12 (rat pheochromocytoma) cells and RT-PCR was set up as reported in *SI Materials and Methods*. To amplify the *Tcte1* transcript, we used primers Tcte1 Fw and Tcte1 Rev (*A*), which amplify a 164-bp fragment spanning exons 2 and 3. Rat adrenal tissue shows as major product a band of smaller size not seen in the other tissues nor in PC12 cells, indicating that *Tcte1* undergoes a tissue-specific alternative splicing.

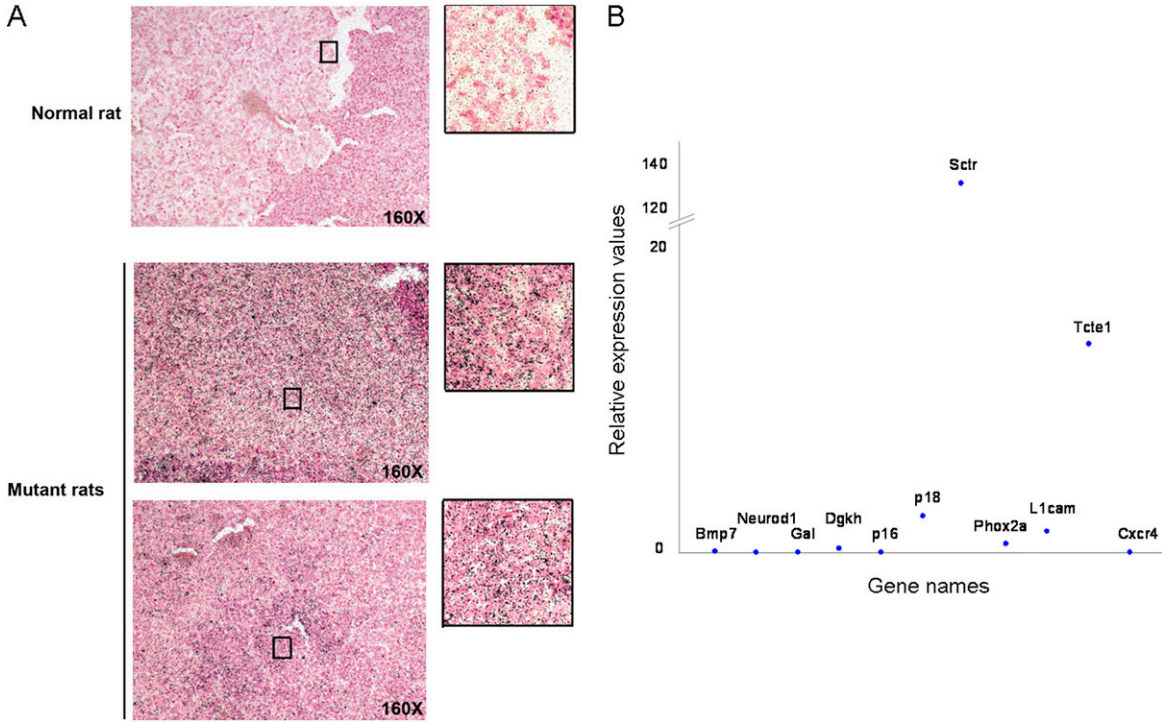

Fig. S4. (*A*) Validation of *Ascl1*/*Mash1* gene overexpression in rat adrenal tumors. In situ hybridization of normal adrenal and two independent adrenal tumor tissues with a probe specific for the *Mash1* transcript. Antisense and sense (negative control) ^{32}P-labeled riboprobes were transcribed from a linearized plasmid containing a partial cDNA for *Mash1* (*Ascl1*, NM_008553). The probes were hybridized overnight on paraffin-fixed tissues sections. Slides were washed and dried and then the signal was revealed by autoradiography. (*B*) Quantitative RT-PCR of selected overexpressed genes in PC12 rat pheochromocytoma cells. The relative mRNA expression level of the target genes was normalized for input RNA using rat β2-microglobulin gene expression (housekeeping gene) and a calibrator rat brain RNA always run in parallel and was calculated with the 2-ΔΔCt formula. The obtained relative value was normalized against normal rat adrenal medulla RNA (control) arbitrarily set to 1. Only few genes up-regulated in MENX adrenal lesions are highly expressed in PC12 cells (i.e., *Sctr*, *Tcte1*, *Cdkn2c*).

Table S1. GO analysis of the most enriched biological process categories for overexpressed genes in rat adrenomedullary lesions

Group	Term	Count	%	*P* value
Hyperplasia				
Functional group 1 median: 3.29E-4	GO:0030182~neuron differentiation	12	6.70	4.91E-05
	GO:0022008~neurogenesis	13	7.26	1.02E-04
	GO:0007399~nervous system development	18	10.06	1.72E-04
	GO:0048699~generation of neurons	12	6.70	1.73E-04
	GO:0007275~multicellular organismal development	32	17.88	1.78E-04
	GO:0032502~developmental process	39	21.79	2.10E-04
	GO:0048856~anatomical structure development	31	17.32	3.18E-04
	GO:0048731~system development	28	15.64	3.29E-04
	GO:0032501~multicellular organismal process	40	22.35	4.86E-04
	GO:0048468~cell development	22	12.29	6.64E-04
	GO:0048869~cellular developmental process	26	14.53	7.60E-04
	GO:0030154~cell differentiation	26	14.53	7.60E-04
	GO:0048513~organ development	22	12.29	9.19E-04
	GO:0050794~regulation of cellular process	33	18.44	4.28E-02
	GO:0009653~anatomical structure morphogenesis	15	8.38	4.92E-02
Functional group 2 median: 1.51E-3	GO:0030182~neuron differentiation	12	6.70	4.91E-05
	GO:0022008~neurogenesis	13	7.26	1.02E-04
	GO:0007399~nervous system development	18	10.06	1.72E-04
	GO:0048699~generation of neurons	12	6.70	1.73E-04
	GO:0007409~axonogenesis	8	4.47	3.53E-04
	GO:0007411~axon guidance	6	3.35	4.12E-04
	GO:0048468~cell development	22	12.29	6.64E-04
	GO:0048666~neuron development	9	5.03	6.78E-04
	GO:0048812~neurite morphogenesis	8	4.47	7.79E-04
	GO:0048667~neuron morphogenesis during differentiation	8	4.47	7.79E-04
	GO:0007417~central nervous system development	9	5.03	9.10E-04
	GO:0000904~cellular morphogenesis during differentiation	8	4.47	1.24E-03
	GO:0051674~localization of cell	11	6.15	1.51E-03
	GO:0006928~cell motility	11	6.15	1.51E-03
	GO:0031175~neurite development	8	4.47	1.63E-03
	GO:0007420~brain development	7	3.91	1.64E-03
	GO:0032990~cell part morphogenesis	8	4.47	5.74E-03
	GO:0048858~cell projection morphogenesis	8	4.47	5.74E-03
	GO:0030030~cell projection organization and biogenesis	8	4.47	5.74E-03
	GO:0016477~cell migration	8	4.47	1.04E-02
	GO:0000902~cell morphogenesis	10	5.59	1.89E-02
	GO:0032989~cellular structure morphogenesis	10	5.59	1.89E-02
	GO:0009653~anatomical structure morphogenesis	15	8.38	4.92E-02
	GO:0009887~organ morphogenesis	7	3.91	1.35E-01
	GO:0009790~embryonic development	3	1.68	6.88E-01
Functional group 3 median: 1.37E-2	GO:0007166~cell surface receptor linked signal transduction	19	10.61	7.32E-03
	GO:0007154~cell communication	35	19.55	1.37E-02
	GO:0007165~signal transduction	30	16.76	3.16E-02
Functional group 4 median: 3.28E-2	GO:0007156~homophilic cell adhesion	5	2.79	6.35E-03
	GO:0022610~biological adhesion	10	5.59	3.28E-02
	GO:0007155~cell adhesion	10	5.59	3.28E-02
	GO:0016337~cell-cell adhesion	5	2.79	9.91E-02
Pheochromocytoma				
Functional group 1 median: 1.16E-2	GO:0007166~cell surface receptor linked signal transduction	20	10.00	5.50E-03
	GO:0007154~cell communication	37	18.50	9.53E-03
	GO:0007186~G protein coupled receptor signaling pathway	12	6.00	1.37E-02
	GO:0007165~signal transduction	32	16.00	2.03E-02
Functional group 2 median: 6.49E-3	GO:0007155~cell adhesion	12	6.00	6.49E-03
	GO:0022610~biological adhesion	12	6.00	6.49E-03
	GO:0016337~cell-cell adhesion	6	3.00	3.71E-02
Functional group 3 median: 3.34E-2	GO:0050808~synapse organization and biogenesis	4	2.00	7.94E-03
	GO:0007416~synaptogenesis	3	1.50	2.98E-02
	GO:0016337~cell-cell adhesion	6	3.00	3.71E-02
	GO:0043062~extracell. structure organization and biogenesis	4	2.00	5.05E-02

Table S1. Cont.

Group	Term	Count	%	*P* value
Functional group 4 median: 6.72E-2	GO:0009966~regulation of signal transduction	10	5.00	1.56E-02
	GO:0051056~regulation of small GTPase mediated signal transduction	5	2.50	3.93E-02
	GO:0046578~regulation of Ras protein signal transduction	4	2.00	6.70E-02
	GO:0007265~Ras protein signal transduction	5	2.50	6.74E-02
	GO:0007266~Rho protein signal transduction	3	1.50	1.72E-01
	GO:0007264~small GTPase mediated signal transduction	6	3.00	2.01E-01
Functional group 5 median: 8.09E-2	GO:0008283~cell proliferation	13	6.50	3.11E-02
	GO:0048519~negative regulation of biological process	15	7.50	7.41E-02
	GO:0048523~negative regulation of cellular process	14	7.00	8.09E-02
	GO:0042127~regulation of cell proliferation	9	4.50	8.62E-02
	GO:0008285~negative regulation of cell proliferation	5	2.50	1.51E-01
Functional group 6 median: 8.29E-2q	GO:0048468~cell development	20	10.00	6.94E-03
	GO:0030154~cell differentiation	24	12.00	7.48E-03
	GO:0048869~cellular developmental process	24	12.00	7.48E-03
	GO:0048856~anatomical structure development	26	13.00	2.60E-02
	GO:0048731~system development	23	11.50	2.86E-02
	GO:0007399~nervous system development	13	6.50	3.55E-02
	GO:0032502~developmental process	32	16.00	5.21E-02
	GO:0007275~multicellular organismal development	25	12.50	5.39E-02
	GO:0016265~death	12	6.00	5.42E-02
	GO:0008219~cell death	12	6.00	5.42E-02
	GO:0032501~multicellular organismal process	33	16.50	8.09E-02
	GO:0006915~apoptosis	11	5.50	8.50E-02
	GO:0012501~programmed cell death	11	5.50	9.11E-02
	GO:0042981~regulation of apoptosis	9	4.50	9.93E-02
	GO:0043067~regulation of programmed cell death	9	4.50	1.06E-01
	GO:0009653~anatomical structure morphogenesis	14	7.00	1.21E-01
	GO:0048513~organ development	15	7.50	1.83E-01
	GO:0006952~defense response	6	3.00	3.12E-01
	GO:0043065~positive regulation of apoptosis	4	2.00	3.83E-01
	GO:0043068~positive regulation of programmed cell death	4	2.00	3.88E-01
	GO:0006955~immune response	4	2.00	7.16E-01
	GO:0002376~immune system process	5	2.50	8.07E-01

Table S2. Clinical characteristics of the human pheochromocytoma patients

Sample ID	Sex	Age	Tumor location*	Tumor size (cm)	Tumor biology	Family history	Gene mutated	Secreted hormone
PGL 65	M	39	A, L	6	Benign	No		n.a.
PGL 95	M	33	A, L	5,2	Benign	No		A
PGL 114	F	72	A, R	5	Benign	No		A
PGL 167	W	32	A, L	18	**Malignant**	No		NA
PGL 172	M	23	A, R	3.2	Benign	No		NA
PGL 174	M	34	A, L	1.8	Benign	No		A
PGL 194	W	28	A, R	5	Benign	No		NA
PGL 227	M	63	A, R	4.1	Benign	No		NA
PGL 246	M	31	A, L	6	Benign	No		A
PGL 295	W	74	A, R	3	Benign	No		NA
PGL 296	M	37	A, L	7	Benign	No		NA
PGL 319	M	70	A, R	6.5	Benign	No		NA
FI 203	F	61	A, R	4	Benign	No		A
FI 220	M	34	A, L	7	Benign	No		NA
FI 248	F	48	A, R	6	Benign	No		NA
FI 251	M	54	A, L	9	Benign	No		NA
FI 317	M	21	A, R	4	Benign	No		NA
FI 326	F	37	A, L	5	Benign	No		NA
FI 333	M	60	A, R	3	Benign	No		A
FI 380	F	40	A, L	3.5	Benign	No		n.a.
FI 383	M	47	A, R	3	Benign	No		A
FI 386	M	59	A, L	3	Benign	No		NA
TB-^{19}F	F	68	A,R	15	**Malignant**	No		n.a.
TB-M44	M	50	A,R	5.5	**Malignant**[†]	No		n.a.
FR 168	M	45	A,R	10	**Malignant**	No		n.a.
PGL 6	F	71	E, Abdominal	5	Benign	No		n.a.
PGL 28	F	62	E, Pararenal	8	Benign	No		none
PGL 29	F	48	E, Abdominal	5	Benign	No		A
PGL 30	M	62	E, Abdominal	18	Benign	No		A
PGL 102	F	59	E, Abdominal	5	Benign	No		A
PGL 130	F	28	E, Abdominal	5	Benign	No		NA
PGL 144	F	36	E, Carotid	3.5	Benign	No		n.a.
PGL 339	M	54	E, Abdominal		Benign	No		A
PL 50	F	51	A, L	5	Benign	Yes	RET-C634R	n.a.
PL 51	F	21	A, R	2.5	Benign	Yes	RET-C634R	n.a.
PL 52[‡]	F	50	A, L tu 1	6	Benign	Yes	RET-C634R	n.a.
PL 53[‡]	F	50	A, L tu 2	7	Benign	Yes	RET-C634R	n.a.
PL 54	F	63	A, L	5.5	Benign	Yes	RET-C620Y	n.a.
PL 55	F	33	A, L	2	Benign	Yes	RET-C634R	n.a.
PL 56[§]	F	27	A, R tu 1	1.5	Benign	Yes	RET-C634R	n.a.
PL 57[§]	F	27	A, L tu 2	2.2	Benign	Yes	RET-C634R	n.a.
PL 58	F	29	A, R	1.3	Benign	Yes	RET-C634R	n.a.
PL 59	F	47	A, L	4	Benign	Yes	RET-C618S	n.a.
PGL 8	F	62	A, L	4	Benign	Yes	SDHD-H50R	NA
PGL 112	F	60	A, R		Benign	Yes (VHL)	not found	NA
PGL 7	M	32	E, Abdominal		**Malignant**	Yes	SDHB-del632G	n.a.

The malignant cases are indicated in bold. Secreted hormones: A, adrenaline; NA, noradrenaline; n.a, not available.
*Location: A, adrenal; L, left; R, right; E, extra-adrenal
[†]Tumor infiltration of the diaphragm.
[‡]The same patient.
[§]The same patient.

Table S3. Quantitative RT-PCR results obtained for the indicated genes on human pheochromocytoma/paraganglioma samples

Sample ID	*GAL*	*DGKH*	*BMP7*	*PHOX2A*	*L1CAM*	*TCTE1*	*EBF3*	*SOX4*	*ASCL1*
PGL 65	++	0	++	++	++	0	0	0	+
PGL 95	+++	+	+	++	++	0	+	+	0
PGL 114	++	+	++	++	++	0	0	++	++
PGL 167	0	++	++	+++	+	0	+++	+	+
PGL 172	+	++	+	+	++	0	+	+	0
PGL 174	+++	0	+	++	++	0	+	0	+
PGL 194	Nd	+	++	+	++	+	Nd	Nd	Nd
PGL 227	0	+	+	+	++	0	++	0	+
PGL 246	0	+	+	+	++	0	+	0	+
PGL 295	0	0	+	+	0	+	0	0	+
PGL 296	+++	0	++	++		0	0	0	0
PGL 319	0	+	+	+	+	0	++	0	0
FI 203	++	0	+	+	+	0	0	0	+
FI 220	0	+	+	+	++	0	+	+	+
FI 248	0	0	0	++	+	+	0	0	0
FI 251	+	+	+	+	+	0	+	0	0
FI 317	0	+	++	++	+	0	++	0	++
FI 326	0	+	+	++	++	0	0	+	+
FI 333	++	0	+	++	+	+	0	0	0
FI 380	+++	0	++	++	++	+	++	+	+
FI 383	0	0	++	++	+	0	+	0	0
FI 386	0	+	0	++	0	+	+	0	++
TB-^{19}F	0	+	0	0	0	0	0	+	0
TB-F44	++	+	+	+	+	+	+	0	0
FR 168	++	+	+	++	+	+	+	+	+
PGL 6	+	+	++	++	++	Nd	+	Nd	++
PGL 28	0	+	++	++	++	0	0	0	0
PGL 29	0	+	+	+++	++	0	0	+	0
PGL 30	0	0	0	0	+	0	++	+	0
PGL 102	+++	+	++	++	++	0	++	+	+
PGL 130	0	+	+	+	+	+	+	0	+
PGL 144	+	++	+	++	++	0	+	0	0
PGL 339	0	++	+	++	+	+	0	+	0
PL 50	0	0	+	++	+	+	++	0	+
PL 51	++	0	++	++	++	0	0	+	0
PL 52	++	0	++	+	+	0	+	0	0
PL 53	0	0	+	+	+	+	0	0	+
PL 54	+++	0	0	0	0	0	0	0	+++
PL 55	+	0	0	++	+	0	++	0	+
PL 56	++	0	+	++	+	0	0	0	0
PL 57	0	0	+	++	+	0	0	0	+
PL 58	+	0	+	+	+	0	++	0	+
PL 59	0	+	0	0	0	0	++	0	0
PGL 8	0	0	++	++	++	0	0	0	0
PGL 112	0	++	++	++	++	0	+	+	++
PGL 7	0	0	0	+	+	++	+	0	0

0, fold-change < 2; +, 2 < fold-change < 10; ++, 10 < fold-change < 100; +++, 100 < fold-change.

Table S4. Immunohistochemical analysis of L1CAM expression in human pheochromocytoma

Sample ID	Tumor location*	Tumor biology	Familiarity	L1CAM Score†
Normal 1‡				0
Normal 2				0
Normal 3				0
PC 22§	A	Benign	Sporadic	3+
PGL 65	A,L	Benign	Sporadic	3+
PGL 95	A,L	Benign	Sporadic	3+
PGL 114	A,R	Benign	Sporadic	3+
PGL 167	A,L	Malignant	Sporadic	2+
PGL 172	A,R	Benign	Sporadic	3+
PGL 174	A,L	Benign	Sporadic	2+
PGL 194	A,R	Benign	Sporadic	3+
PGL 227	A,R	Benign	Sporadic	2+
PGL 246	A,L	Benign	Sporadic	2+
PGL 295	A,R	Benign	Sporadic	2+
PGL 296	A,R	Benign	Sporadic	3+
PGL 8	A,L	Benign	SDHD-H50R	2+
PGL 112	A,R	Benign	VHL?	2+
PGL 6	E, Abdominal	Benign	Sporadic	1+
PGL 28	E, Pararenal	Benign	Sporadic	2+
PGL 29	E, Abdominal	Benign	Sporadic	0
PGL 102	E, Abdominal	Benign	Sporadic	3+
PGL 144	E, Abdominal	Benign	Sporadic	3+
PG 3§	E, Abdominal	Benign	Sporadic	2+
PG 15	E, Abdominal	Benign	Sporadic	3+
PG 17	E, Abdominal	Benign	Sporadic	3+
PG 19	E, Abdominal	Benign	Sporadic	3+

*Tumor location as reported in Table S1.
†Score was given following the established DAKO Scoring for HER2/Neu in breast cancer patients.
‡Normal means normal human adrenal medulla.
§Case PC22 and the four PG cases have been previously described in Pellegata et al. (1).

1. Pellegata NS, et al. (2007) Human pheochromocytomas show reduced p27Kip1 expression that is not associated with somatic gene mutations and rarely with deletions. *Virchows Arch* 451:37–46.

Other Supporting Information Files

Dataset S1 (XLS)
Dataset S2 (XLS)